RADIATION RESEARCH **165**, 240–247 (2006)
0033-7587/06 $15.00

TECHNICAL ADVANCE

Dosimetry for Quantitative Analysis of the Effects of Low-Dose Ionizing Radiation in Radiation Therapy Patients

Joerg Lehmann,[a,b,1] Robin L. Stern,[b] Thomas P. Daly,[a] David M. Rocke,[c] Chad W. Schwietert,[b] Gregory E. Jones,[d] Michelle L. Arnold,[a] Christine L. Hartmann Siantar[a,b] and Zelanna Goldberg[b]

[a] *Glenn T. Seaborg Institute, University of California–Lawrence Livermore National Laboratory, Livermore, California;* [b] *Department of Radiation Oncology, University of California Davis Cancer Center, Sacramento, California;* [c] *Division of Biostatistics and Department of Applied Science, University of California Davis Cancer Center, Sacramento, California; and* [d] *Hazards Control and Safety Program, University of California–Lawrence Livermore National Laboratory, Livermore, California*

Lehmann, J., Stern, R. L., Daly, T. P., Rocke, D. M., Schwietert, C. W., Jones, G. E., Arnold, M. L., Hartmann Siantar, C. L. and Goldberg, Z. Dosimetry for Quantitative Analysis of the Effects of Low-Dose Ionizing Radiation in Radiation Therapy Patients. *Radiat. Res.* 165, 240–247 (2006).

We have developed and validated a practical approach to identifying the location on the skin surface that will receive a prespecified biopsy dose (ranging down to 1 cGy) in support of *in vivo* biological dosimetry in humans. This represents a significant technical challenge since the sites lie on the patient's surface outside the radiation fields. The PEREGRINE Monte Carlo simulation system was used to model radiation dose delivery, and TLDs were used for validation on phantoms and for confirmation during patient treatment. In the developmental studies, the Monte Carlo simulations consistently underestimated the dose at the biopsy site by approximately 15% (of the local dose) for a realistic treatment configuration, most likely due to lack of detail in the simulation of the linear accelerator outside the main beam line. Using a single, thickness-independent correction factor for the clinical calculations, the average of 36 measurements for the predicted 1-cGy point was 0.985 cGy (standard deviation: 0.110 cGy) despite patient breathing motion and other real-world challenges. Since the 10-cGy point is situated in the region of high-dose gradient at the edge of the field, patient motion had a greater effect, and the six measured points averaged 5.90 cGy (standard deviation: 1.01 cGy), a difference that is equivalent to approximately a 6-mm shift on the patient's surface.

INTRODUCTION

The significance of the biological activity of low-dose ionizing radiation in the range of 1–10 cGy is a subject of contention. While there is ample evidence from *in vitro* cell culture models that doses as low as 1 cGy result in changes in the transcriptome (*1*), the cells used in such studies lack the complexity of three-dimensional tissue. In addition, cell lines are immortalized or transformed and live on artificial substrates. Thus, to develop rational, scientifically sound public policy on safe low-dose exposures, it is necessary to obtain data directly in humans. While it is not possible to irradiate volunteers prospectively for the purpose of such studies, humans are irradiated daily for the treatment of cancer. These patients can be a study population if the physics and dosimetry of their treatment plans can be made sufficiently robust to prospectively identify sites of low-dose exposure from which tissue samples can be obtained (*2*). Since the doses of interest in support of public policy are well below those used in therapy (1–10 cGy and 2 Gy, respectively) and the treatment plans are essentially fixed by therapeutic strategy (multiple-beam, conformal treatment portals), the dosimetry is complex. Low-exposure points are outside of the treatment portal, an area that is insufficiently modeled in standard treatment planning systems (*3–20*). We therefore used a Monte Carlo treatment planning system for this study.

We have designed, validated and implemented a research protocol to identify the location of biopsy points on the volunteer patient's skin surface with a dosimetric uncertainty of 15% or better, which is well within the acceptable uncertainty for support of clinical/biological studies.

MATERIALS AND METHODS

Monte Carlo System

The PEREGRINE Monte Carlo system was chosen for the study (*21*). A research version of the system was commissioned to simulate the 18 MV beam of a Varian Clinac 2100C (Varian Medical Systems, Palo Alto, CA) at the UC Davis Cancer Center. Simulation parameters and machine specific calibration methods are described in detail in ref. (*21*). In brief,

[1] Address for correspondence: UC Davis Cancer Center, 4501 X Street, Suite G 140, Sacramento, CA; e-mail: lehmann@ucdavis.edu.

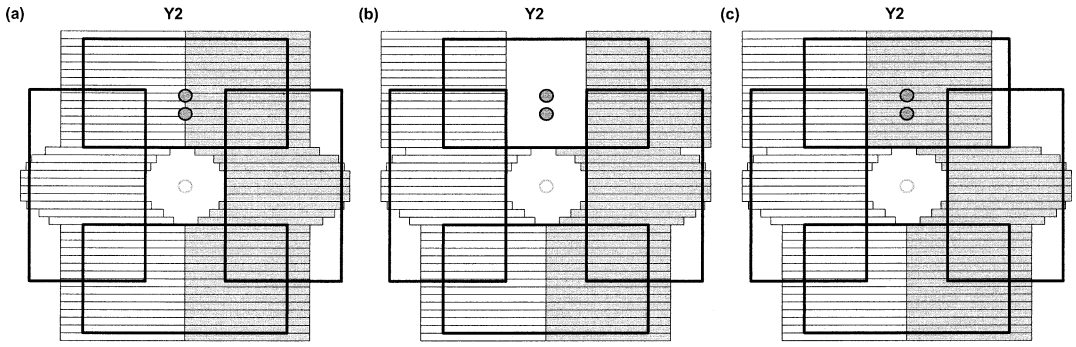

FIG. 1. Schematic of an MLC shaped field with (panel a) the MLC leaves closed under the Y2 jaw in standard 0,0 position, (panel b) the MLC leaves open under the Y2 jaw, and (panel c) the MLC leaves set to −7,7 under the Y2 jaw to avoid abutting the leaves directly over the points of interest (filled circles).

the head of the linear accelerator from the top of the Bremsstrahlung target to the bottom of the monitor chamber has been modeled using the BEAM software (*22*). Accelerator components that are in the path of the primary beam (target, primary collimator, flattening filter, monitor chamber) were included in the treatment head simulation. Components outside the primary beam path such as the treatment head shielding were not considered in the simulation. Particles that entered these regions were terminated and their contributions ignored. Dimensions and material properties are based on manufacturer's information and were fine-tuned with phantom measurements. After the accelerator had been successfully reproduced in the BEAM code, a beam model (*23*) was created that was the basis for the PEREGRINE simulations including those performed in this study. The commissioning of the source model for this accelerator was reported in ref. (*21*). In the PEREGRINE simulations, the remaining accelerator components in the path of the primary beam were modeled (jaws and Multileaf Collimators, MLCs), as well as the phantom or patient based on a computed tomography (CT) scan. The simulations were run in the ''full physics'' mode, which included a full physics transport through realistically shaped jaws and MLCs as described previously (*21*). The simulation parameters used were: ECUT = 0.521 MeV, PCUT = 0.010 MeV. Simulations were performed until a statistical uncertainty of 0.28% was reached at the voxel with the highest dose. The statistical uncertainty of the dose at the selected points depended on their location. Generally, the further out of field a point is located, the lower the dose is and the larger the uncertainty. The average uncertainty was 1.7%.

Selection of Beam Shaping Mechanism

Since the points of dose interest were located beyond the field boundaries, the method of field shaping needed to be addressed. While the jaws function as the major field shaping tool, there are two options for the secondary field shaping tools at our clinic: Cerrobend® blocks and MLCs. Blocks shape the radiation field within the rectilinear region described by the jaws. They normally extend only slightly beyond this region, under the jaws. Since the dose points of interest are located under the jaw, the outside edge of a block would have to be modeled precisely in the Monte Carlo code. This is not practical because the blocks are made individually and the position and shape of their outer edge vary slightly from case to case. Another option would be to extend the block to cover the area of interest completely, thus eliminating the influence of its outer edge. This proved not to be viable either, since block weight became excessive and the production tolerances were prohibitively high. MLCs are very reproducible, but Varian's MLC has gear mechanisms and movable banks in the direction of leaf travel that are very difficult to model. Therefore, we chose to locate the biopsy points outside the field perpendicular to the MLC leaf travel direction. For the treatment site in the initial study, this was possible without affecting the overall patient treatment strategy.

While the positions of the leaves within the field were dictated by the treatment plan, there are multiple options for those leaves not involved in field shaping. Of special interest were those leaves under the Y2 jaw,[2] since the dose points of interest are under that jaw. Due to the construction of the MLC, those leaves could not be completely retracted (i.e. be in the ''parked'' position). The standard position for them usually defaults to be ''closed'', abutting at the center line of the field axis (see Fig. 1a). This position was not desirable for our measurements because we wanted to position the biopsy points along this axis to simplify their identification on the patient. Dose accuracy to the degree necessary for studying low-dose radiation at the doses discussed here is difficult to achieve in the simulation under abutting rounded-edge MLC leaves, due to the positioning uncertainty of the leaves. Two more favorable scenarios are shown in Fig. 1b and c. Here the MLC leaves under the Y2 jaw are either open, that is, all leaves are set to 7 cm from central axis (Fig. 1b), or they are closed but abut away from the field axis, i.e., the MLC pairs are set to ''−7, 7'' (Fig. 1c). Since we did not find any dosimetric advantage in the open case, and it gives slightly more radiation to the patient, we used the MLC closed position (Fig. 1c) for our studies.

Beam Direction and Biopsy Site Location

Within a solid tissue-equivalent material, the radiation dose inside the field deposited from a megavoltage photon beam, starting at the material surface, rises with depth and then reaches a plateau followed by a gradual falloff. The rise is caused by the establishment of transient charged-particle equilibrium and the falloff by attenuation and scattering of the primary beam. The dose plateau is generally a preferred location for accurate radiation dosimetry and would also serve well for biopsy locations. Using tissue-equivalent bolus material, the plateau can be moved to the accessible skin level. Outside the beam, however, such a dose plateau does not exist, since most radiation contributing to the dose is scattered radiation coming from different directions. Using Monte Carlo simulations and measurements in water-equivalent slab phantoms, we found a more favorable depth–dose profile at the location where the beam exits the solid material. We therefore used the beam exit as the site for the biopsies (i.e., a posterior beam for biopsy on the patient's anterior skin). We also used simulations to investigate the effect on the dose of establishing electron equilibrium at the exit surface by adding increasing thicknesses of bolus material. We found that after 2.5 cm of tissue-equivalent material (bolus), no more change in dose was observed at the material (skin) surface. Thus a 3-cm-thick bolus material over the biopsy site was chosen for patient studies.

[2] MLC leaf positions are described according to the Varian convention: The first number corresponds to the position of the leaf of the leaf bank A (under X1 jaw) and describes the position of this leaf as the distance of its tip from the field midline in the projection to the isocenter plane in centimeters. The second number describes the leaf of the leaf bank B (under X2 jaw) accordingly. Negative numbers indicate overtravel, which is a leaf crossing the midline.

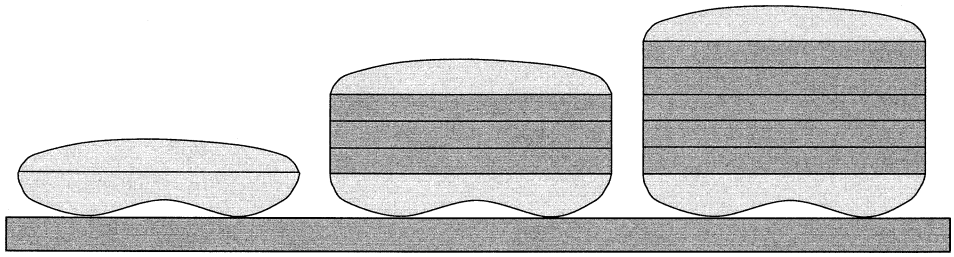

FIG. 2. Custom anthropomorphic phantom with variable thickness. Shown are the thinnest (left) and the thickest (right) version and one in between configuration. The phantom is described in more detail in ref. (*24*).

Confirmatory Measurements with TLDs

Thermoluminescence dosimeters (TLDs) were chosen for the empirical validation of the results of Monte Carlo simulations outside the treatment field. TLDs have the advantage of being sensitive and accurate down to 1 cGy. Using square TLDs with a side length not larger than the diameter of our biopsy core avoided dose averaging, which could be significant in the areas of steep dose gradient. TLD type EXT-RAD 740 (Harshaw–Thermo RMP, Solon, OH) were used for this study. This model uses a single ^{7}LiF:Mg,Ti chip (3×3 mm^2, TLD-700 material) permanently mounted on a bar-coded substrate. The chip thickness is 40 mg/cm^2, which corresponds to approximately 0.1 mm. The TLD chip-strate is loaded into a sealed pouch with a 0.008-inch-thick window over the active portion of the TLD. Since the window is very thin, the position of the chip-strate can be identified easily and accurately through it. The TLDs were read using a Harshaw model 6600 automatic TLD reader. We calibrated the TLDs through comparative measurements in a water-equivalent slab phantom. These measurements were performed inside and outside the field at various depths (3.2 cm, 30 cm, 40 cm). Absolute dose was measured with a calibrated Farmer chamber that had been shown to be uniform in response from therapeutic energies down to 150 kVp with an increased response of 2.5% at 60 kVp per calibration report from The University of Wisconsin Radiation Calibration Laboratory. The TLDs were used both for experimental verification of our calculation methods and to verify the dose given to the patient at the biopsy site(s).

Validation of Accuracy of Monte Carlo System

A newly designed anthropomorphic phantom (*24*) was used to investigate the accuracy of the PEREGRINE Monte Carlo system in predicting the dose outside of the treatment field for a single beam and for multiple beams as used in patient treatment. The phantom was produced in cooperation with the manufacturer of the RANDO® Phantoms (The Phantom Laboratory, Greenwich, NY). It has adjustable body thickness to enhance the verification by more closely simulating the variation in actual patient body size. Since the intra-phantom scatter is an important contributor to the peripheral dose (*16*), the thickness of the patient was recognized to be important and worth investigating. A more detailed description of the new phantom (Fig. 2) can be found elsewhere (*24*).

In initial investigations, the ability of the PEREGRINE Monte Carlo system to correctly simulate dose outside of the field of a single beam was determined. Results of TLD measurements in the anthropomorphic phantom were compared to Monte Carlo simulations, which were based on CT images of the phantom with the bolus as described above. The TLDs were positioned on the anterior side of the phantom at variable distances from the field edge under the bolus material to span the anticipated biopsy locations (2, 8, 10, 12 cm from central beam axis). All TLD measurements were repeated three times within a measurement series, and two to three measurement series were done for every phantom thickness-beam setup combination. Therefore, at least six independent TLD measurements were performed per data point. Overall, the average standard deviation for one measurement series was 3.5%. The beam was applied from the posterior side of the phantom, putting the measurement points on the beam exit side. Measurements were performed for four different phantom thicknesses (17.9 cm, 25.4 cm, 28.1 cm, 30.7 cm). An open beam (field size 10×10 cm^2, MLC parked) and an MLC shaped beam were investigated. For the latter, a realistically shaped MLC field was used. The MLC leaves under the Y jaws were closed and abutted on the side (similar to Fig. 1c).

Next, multiple beams conditions were verified using the anthropomorphic phantom. Five isocentric treatment fields (gantry angles: 70, 120, 240, 290 and 360°, Varian convention) were directed at the phantom with the isocenter positioned about mid-phantom. The beam setup closely resembled the radiation treatment of the patient volunteers. The same beam angles, beam energy, and relative monitor units were used. The fields were realistically shaped using the MLC. The MLC leaves under the Y jaws were closed and abutted on the side (similar to Fig. 1c). Measurements were again performed for four different phantom thicknesses using TLDs placed at 2, 8, 10 and 12 cm from central beam axis and compared to Monte Carlo simulations based on CT images of the phantoms.

A detailed statistical analysis was performed to investigate any dependence of the difference between simulation results and measurements on phantom thickness and on distance from the central beam axis (and from field edge). For the analysis, the mean dose reading from the TLDs was used without adjustment for the number of TLDs, since the variability across experiments is greater than the variation across replicates. Uncertainties were derived from residual statistical modeling error, regardless of the variability within replicates and the predicted statistical uncertainty of the PEREGRINE Monte Carlo calculations. The natural logarithm of the ratio of the predicted dose (Monte Carlo simulation) to the measured dose (TLD) was evaluated in an analysis of variance.

Patient Studies

Men undergoing radiation therapy for treatment of their localized prostate cancer consented to the study (institutional review board approved). The men received an extra CT scan with bolus covering the anterior side of the treatment region and extending in the superior direction. Based on this CT scan, a treatment plan similar to the patient's regular plan was created using a clinical 510K-cleared treatment planning system and approved by the treating physician. All patients were treated with 18 MV X rays. The prescription dose was 2 Gy to the 95% isodose line, with 100% at isocenter. The plan was then submitted for Monte Carlo simulation. After the simulation, the positions of the dose points of interest on the skin were identified. The patient volunteers had biopsies at the 1-cGy and/or the 10-cGy point(s), depending on their group within the research protocol. The sites for biopsy were located and marked on the first day of treatment while the patient was in treatment position. A TLD was placed on the position of each biopsy site and another one immediately adjacent to it. TLDs were removed after treatment for readout. As detailed elsewhere (*2*), biopsies were obtained after the first fraction of the patient's radiation treatment.

Sixteen patients were irradiated. Since each patient has multiple biopsy points, a total of 42 measurement points were taken.

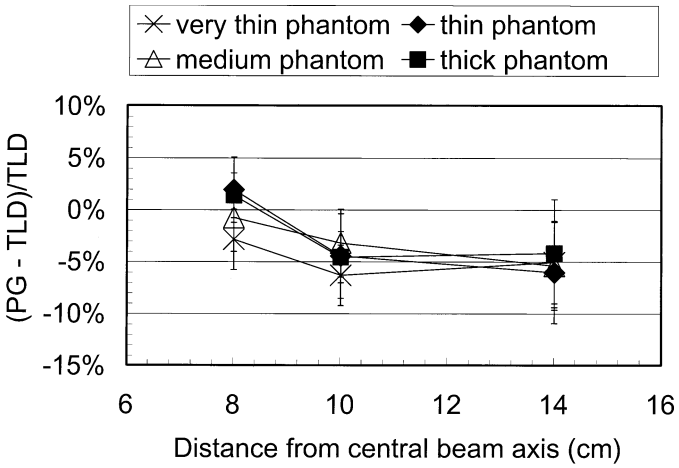

FIG. 3. Comparison of the phantom measurements with the corresponding Monte Carlo simulations for a single open beam (isocentric setup, 10 × 10 cm², MLC parked) for four phantom configurations: very thin (17.9 cm thick), thin (25.4 cm), medium (28.1 cm) and thick (30.7 cm). The *y* axis shows the percentage difference between simulations (PG) and TLD measurements (TLD): (PG − TLD)/TLD. The *x* axis represents the distance of measurement point from the central beam axis (CAX). The error bars represent one standard deviation.

RESULTS

Single-Beam Validation of PEREGRINE

The agreement of the phantom measurements for a single open beam (10 × 10 cm², MLC parked) with the corresponding Monte Carlo simulations is shown in Fig. 3. The difference in Monte Carlo simulation and measurement is plotted as a function of distance of measurement point from the central beam axis for four phantom thicknesses. Three of the thicknesses (25.4 cm, 28.1 cm, 30.7 cm) represent the range of anterior-posterior thicknesses of realistic prostate cancer patients. The thinnest version of the phantom (17.9 cm thickness, left-most drawing in Fig. 2) is not clinically relevant and was examined only to gain insight into simulation-measurement deviation trends. The error bars in Fig. 3, as well as in Figs. 4 and 5, represent the propagated uncertainty from measurement and Monte Carlo simulation expressed as one standard deviation.

For the measurement points outside the field, as shown in Fig. 3, doses obtained with Monte Carlo simulations are generally smaller than measured doses, resulting in a negative difference as defined here. For off-axis locations greater than 8 cm, the difference is on average −5%. At 8 cm off-axis, the agreement is within 3%, and at a control point inside the field (2 cm of central beam axis, not shown here), the agreement is better than 2%. The observed trend of increasing difference between simulation and measurement with increasing distance from the central beam axis, and thereby from the field edge, proved to be statistically significant ($P = 0.0083$).

With a single MLC shaped beam (as in Fig. 1c), the deviation of off-axis simulations from measurements was greater than in the open-beam case. The relationship between the deviation and the distance from the central beam axis is shown in Fig. 4a. The trend of increasing deviation with distance was found to be significant ($P = 0.0161$). There was no significant correlation between phantom thickness and measurement deviation from Monte Carlo predictions ($P = 0.24$) (Fig. 4b).

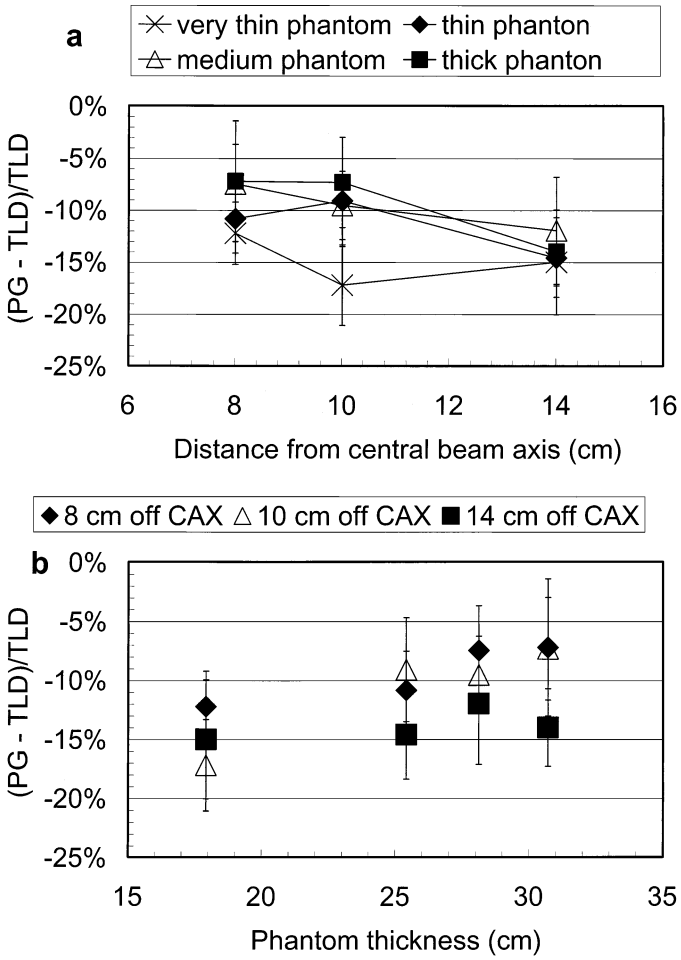

FIG. 4. Comparison of the phantom measurements with the corresponding Monte Carlo simulations for a single MLC shaped beam (isocentric setup, 10 × 10 cm², MLC leaves under the jaws closed on the side as in Fig. 1c) for four phantom configurations: very thin (17.9 cm thick), thin (25.4 cm), medium (28.1 cm) and thick (30.7 cm). The *y* axis shows the percentage difference between simulations (PG) and TLD measurements (TLD): (PG − TLD)/TLD. The percentage difference is plotted as a function of distance of the measurement point from the central beam axis (CAX) for the four phantom thicknesses (panel a) and as a function of phantom thicknesses for three distances of the measurement point from the central beam axis (panel b). The error bars represent one standard deviation.

Multiple-Beam Validation of PEREGRINE

To use PEREGRINE to determine the out-of-field dose in clinical treatment plans, its out-of-beam accuracy for multiple coplanar beams had to be verified. Figure 5 shows deviations for five-beam cases, where four oblique beams are added to the one PA beam as described in the previous paragraph. All beams are MLC-shaped for a standard pros-

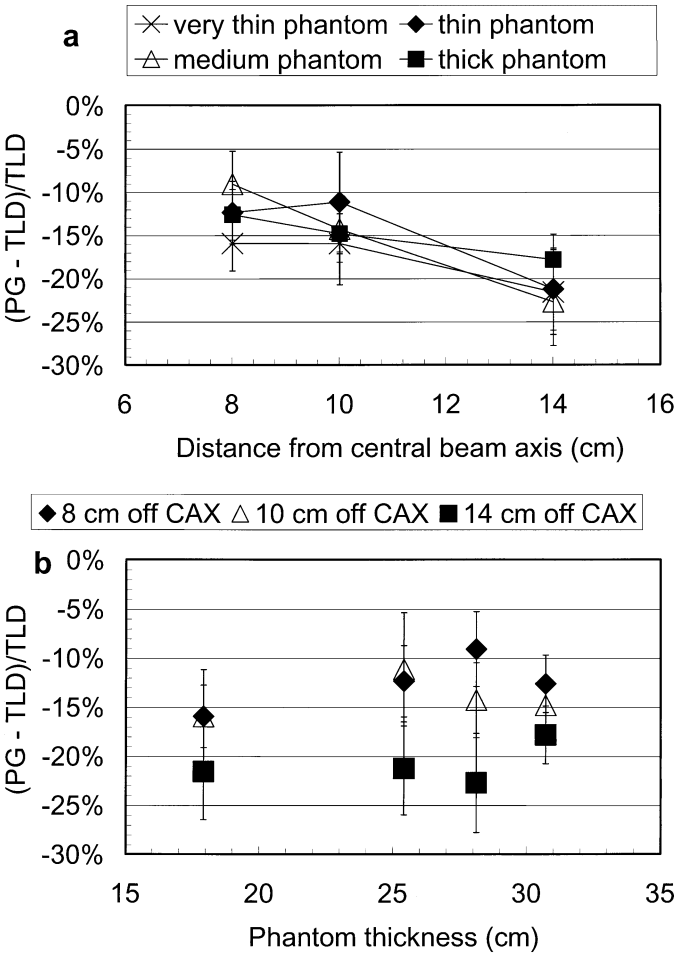

FIG. 5. Comparison of the phantom measurements with the corresponding Monte Carlo simulations for a realistic five-beam prostate treatment (isocentric setup, 10 × 10 cm², MLC leaves under the jaws closed on the side as in Fig. 1c) for four phantom configurations: very thin (17.9 cm thick), thin (25.4 cm), medium (28.1 cm) and thick (30.7 cm). The *y* axis shows the percentage difference between simulations (PG) and TLD measurements (TLD): (PG − TLD)/TLD. The percentage difference is plotted as a function of distance of measurement point from the central beam axis (CAX) for the four phantom thicknesses (panel a) and as a function of phantom thicknesses for three distances of the measurement point from the central beam axis (panel b). The error bars represent one standard deviation.

tate cancer treatment in the way illustrated in Fig. 1c. These additional beams increase the deviation of the Monte Carlo simulations from the measurements to approximately 8–22% with a trend of increasing deviation with distance from the central beam axis ($P = 0.0264$). Figure 5a illustrates this dependence of the deviation on the distance of the measurement point from the central beam axis. Figure 5b shows the relationship between the phantom thickness and the percentage deviation of the Monte Carlo simulation and the measurements. For five-field cases, thickness dependence of the deviation also was not observed ($P = 0.97$).

Patient Measurements

A single correction factor of 1.18 was used in support of the clinical trial dosimetry. The phantom measurements had demonstrated that patient thickness would not affect the dosimetric predictions. While there was a statistical relationship to distance from the field edge, the practical application of this was thought to be of minor significance. It was recognized that the 10-cGy point was going to lie in the high-dose gradient region where the variance due to patient breathing motion (*25, 26*) and minor setup inaccuracies would greatly overwhelm the Monte Carlo limitations.

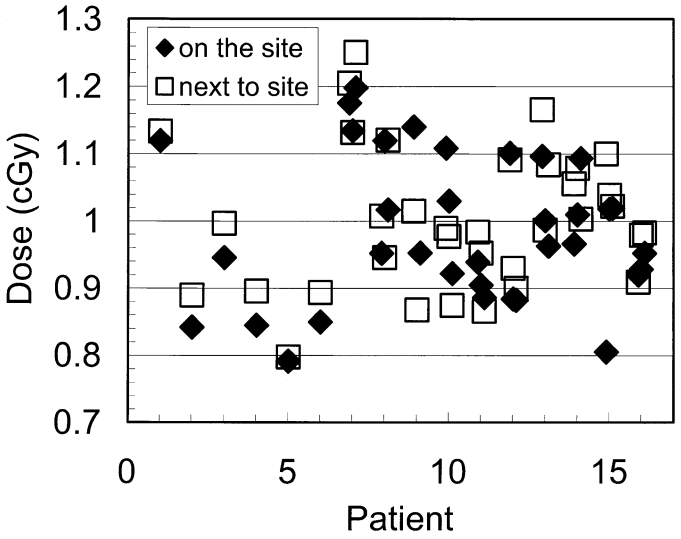

FIG. 6. TLD measurements at locations on patients that were preselected to receive 1 cGy (filled diamonds) and adjacent to the locations (open squares). Patients 1–6 each had one 1-cGy biopsy location; patients 7–16 each had three locations. Average dose on the location was 0.985 cGy (standard deviation: 0.110 cGy) and adjacent to the location was 1.00 cGy (standard deviation: 0.105 cGy). Based on the repeatability in the TLD phantom measurements, the average uncertainty of TLD measurements is 3.6% (1 SD).

Figure 6 shows the dose measured at the predicted 1-cGy biopsy points in 16 (consecutive) patients. The average dose measured with the TLD on the biopsy location predicted by the corrected Monte Carlo algorithm to receive 1 cGy was 0.985 cGy (standard deviation: 0.110 cGy). The additional TLD adjacent to the biopsy location measured on average 1 cGy (standard deviation: 0.105 cGy).

The 10-cGy point represents a greater dosimetric challenge since the points are located within a high-dose gradient region as described above. For the six patients that underwent biopsies at the 10-cGy point, the average measured dose at the location of the biopsy was 5.90 cGy (standard deviation: 1.01 cGy) and adjacent to the location 5.84 cGy (standard deviation: 1.80 cGy) (see Fig. 7).

DISCUSSION

Translational human data are essential in the development of scientifically sound public policy regarding health risks of low-dose ionizing radiation in on humans. The methodological developments that we have described above are the first to our knowledge to use Monte Carlo simula-

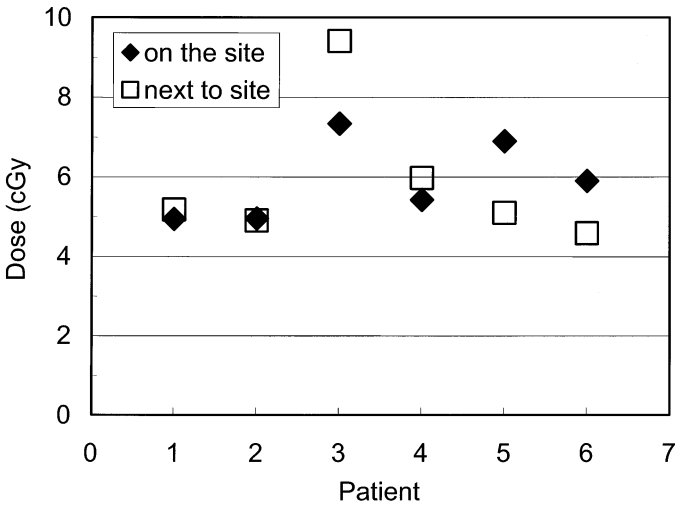

FIG. 7. TLD measurements at locations on patients that were preselected to receive 10 cGy (filled diamonds) and adjacent to the locations (open squares). Average dose on the location was 5.90 cGy (standard deviation: 1.01 cGy) and adjacent to the location 5.84 cGy (standard deviation: 1.80 cGy). As described for Fig. 6, the average uncertainty of TLD measurements is 3.6% (1 SD).

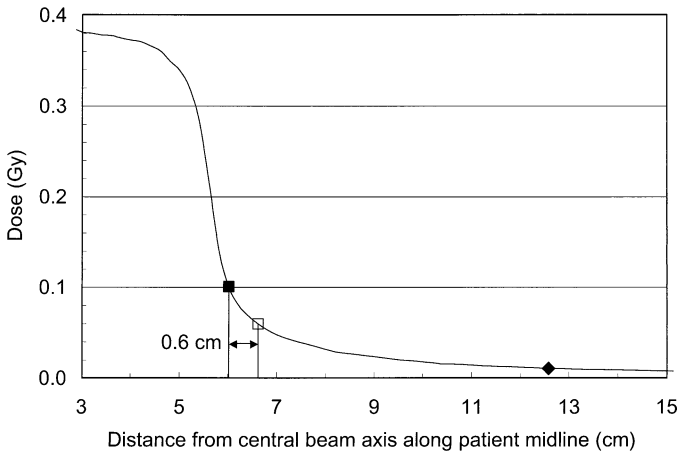

FIG. 8. Dose along the midline of a typical patient under the bolus material from a single prostate treatment (2 Gy at 95% isodose line). The 1-cGy point (diamond) is located in a low-gradient area well outside the field. The 10-cGy point (filled square) is at the edge of the field in a very steep dose gradient. The average measurement for the 10-cGy points (Fig. 7) was 5.9 cGy (open square), which for this typical case is about 6 mm away from the location with the desired 10 cGy.

tions in real-world conditions in support of these types of studies. We have now implemented a practical, usable protocol for out-of-beam, low-dose region dosimetry at the skin surface at sites that receive 1 cGy, or 0.5% of a standard therapeutic radiation treatment dose of 2 Gy. The 10-cGy locations are less accurately described for the investigated patient group, because in their treatment plans the 10-cGy locations are found at the field edge where a steep dose gradient is present. In principle, however, the method described is capable of locating 10-cGy points with even greater accuracy than 1-cGy points since the dose is higher and the uncertainties are therefore smaller.

While this methodology is sufficiently accurate to support the clinical/biological investigations, the comparison of Monte Carlo simulations to measurements has revealed discrepancies of the order of 15%. Similar deviations had been observed before for a simpler slab phantom geometry, where out-of-field underestimations by PEREGRINE of up to 15% in comparison with measurements were found (*21*). Our investigations of a realistic treatment situation with an anthropomorphic phantom showed that outside the field dose calculation with Monte Carlo simulations are also generally lower than measurements using TLDs. This is true even for the simplest case of a single open beam (with parked MLC), with measurements taken on the beam exit side of the phantom. The effect is noticeable starting between 8 and 10 cm from the central beam axis (10×10-cm^2 field). The deviation increases for an MLC shaped beam and even more for a five-beam treatment using the MLC. The average deviation is larger as distances increase from the central beam axis. This trend is statistically significant for all cases examined. No significant influence of the phantom thickness on the deviation of simulation from measurement was observed.

Doses of interest in this study lie in the peripheral region of the radiation field. The radiation transport in the Monte Carlo code is modeled well in the main beam line starting at the exit window of the electron acceleration structure. Components outside the main beam line are not as well defined in the simulation, and therefore dose components associated with them are subject to inaccuracy. The sources of dose in the peripheral area are (a) leakage from the treatment unit, (b) scatter from the primary collimator and the flattening filter, (c) scatter from the secondary collimators and from beam modifiers such as wedges, blocks and the MLCs, and (d) internal scatter originating in the patient. This suggests that the discrepancy between simulation and validation measurement stems at least in part from simplifications in the simulation of the accelerator head. With the addition of the MLCs to the beam shaping and simulations, problems may also arise from the simulation of either the MLC transmission properties and/or scatter off the MLCs into regions outside the field. Our results with the five-beam case (four oblique beams added) show larger deviations, which may be originating from additional head scatter that is not accounted for in the simulations and that suffers less intra-phantom attenuation to diminish its impact, compared to the single PA beam in the first two setups.

While the addition of an empirical adjustment factor resulted in highly accurate identification of the 1-cGy biopsy point, 10-cGy points are harder to prespecify since they are located in the high-dose gradient of the field edge. This is illustrated in Fig. 8, which shows the dose along the midline of a patient under the bolus material for a single prostate treatment fraction (2 Gy at 95% isodose line). The 1-cGy point (filled diamond) is located in a low-gradient area

well outside the field while the 10-cGy point (filled square) is at the edge of the field in a very steep dose gradient. Considering the circumstances of a clinical radiation treatment, including the fact that the patient is breathing, small movements of the biopsy site throughout the treatment cannot be avoided. For the 10-cGy point, such small movements result in significant dosimetry uncertainties. As illustrated in Fig. 8, moving the point on the skin by just 6 mm causes the dose received to drop to the measured average of 5.9 cGy (open square). Under these real-world conditions, uncertainties in identifying the biopsy site on the patient and, although small, uncertainties in the setup of the patient have a similarly large impact. However, although a 6-mm uncertainty in patient alignment would account for the deviations found, the fact that we found a consistently lower dose with the TLD over the six patients observed and also in subsequent additional measurements rules out the random nature of this phenomenon. Therefore, additional problems with the accuracy of the Monte Carlo simulation at the field edge cannot be excluded, since small errors in the geometrical description of the machine (i.e. shape and size of the edge of the jaw or MLC leaves) can result in significant changes in predicted dose. However, even if the Monte Carlo code problems at this challenging location were completely resolved, the observed high sensitivity to small spatial uncertainties remains. Thus the Monte Carlo CT-based method of dose prediction presented here is not sufficient in itself to operate in such dose gradients. A modification of the protocol to address this challenge is under development. However, at the 1-cGy point, the present method delivers accuracy with high reliability and has allowed important biological studies to proceed.

An 18 MV photon beam has known contamination by photoneutrons that needs to be considered in the analysis of the biological data. Accounting for neutron dose is complicated by the fact that the quality factors for neutron radiation are still under debate. Verification measurements that we performed at our beam, similar to those in the literature (*27–30*), with CR-39 foils demonstrated that the neutron dose is approximately 0.1 cSv at the location of our biopsies. This amounts to 10% of the photon dose at the 1-cGy location and will be taken into account in the analysis of the biological data. It is, however, low enough that it will not preclude this approach to biopsy collection. The measurements with the TLD-700 used in the phantom and patient measurements are not affected by the neutron dose, since TLD-700 are insensitive to neutrons. The Monte Carlo system used in the study only transports photons and electrons, not neutrons.

The methodology we have developed and described herein represents a new approach and a step forward in the implementation of technology in support of biological evaluations of human subjects undergoing standard radiation therapy. While clinical implementation of such technology is never as precise as phantom models suggest, our methodology has allowed us to proceed with clinical trials while continuing to obtain and analyze dosimetric information for the improvement of the Monte Carlo code.

ACKNOWLEDGMENTS

This work was performed under the auspices of the U.S. Department of Energy by University of California Lawrence Livermore National Laboratory under contract No. W-7405-Eng-48 and supported in part by the Office of Science (BER), U.S. Department of Energy, Grant No. DE-FG03-01ER63237. This work has been presented in part at the ASTRO 44th Annual meeting, New Orleans, 2002, the World Congress of Medical Physics and Biomedical Engineering, Sydney, 2003, and the 12th International Conference on Radiation Research in Brisbane, 2003. The authors would like to thank Cynthia A. Fix of LLNL for her support in preparing and reading out the TLD.

Received: September 7, 2004; accepted: August 19, 2005

REFERENCES

1. S. A. Amundson, K. T. Do and A. J. Fornace, Jr., Induction of stress genes by low doses of gamma rays. *Radiat. Res.* **152**, 225–231 (1999).
2. Z. Goldberg, C. W. Schwietert, R. L. Stern, M. Arnold, C. L. Hartmann Siantar, M. A. Descalle and B. E. Lehnert, Exposure to low dose (1–10 cGy) ionizing radiation: Assessment of effects in humans and relevance to cancer. *Int. J. Radiat. Oncol. Biol. Phys.* **54**, 53 (2002).
3. B. A. Fraass and J. van de Geijn, Peripheral dose from megavolt beams. *Med. Phys.* **10**, 809–818 (1983).
4. P. H. van der Giessen, Calculation and measurement of the dose at points outside the primary beam for photon energies of 6, 10, and 23 MV. *Int. J. Radiat. Oncol. Biol. Phys.* **30**, 1239–1246 (1994).
5. M. Stovall, C. R. Blackwell, J. Cundiff, D. H. Novack, J. R. Palta, L. K. Wagner, E. W. Webster and R. J. Shalek, Fetal dose from radiotherapy with photon beams: Report of AAPM Radiation Therapy Committee Task Group No. 36. *Med. Phys.* **22**, 63–82 (1995).
6. R. L. Stern, Peripheral dose from a linear accelerator equipped with multileaf collimation. *Med. Phys.* **26**, 559–563 (1999).
7. S. Sherazi and K. R. Kase, Measurements of dose from secondary radiation outside a treatment field: Effects of wedges and blocks. *Int. J. Radiat. Oncol. Biol. Phys.* **11**, 2171–2176 (1985).
8. S. C. Sharma, J. F. Williamson, F. M. Khan and C. K. Lee, Measurement and calculation of ovary and fetus dose in extended field radiotherapy for 10 MV x rays. *Int. J. Radiat. Oncol. Biol. Phys.* **7**, 843–846 (1981).
9. A. Sanchez-Reyes, M. Ginjaume, H. Chakkor, A. Melero, F. Pons and X. Ortega, Estimation of peripheral dose from two linacs: Mevatron MX6700 and Mevatron KDS. *Med. Dosim.* **19**, 83–87 (1994).
10. J. Novotny and M. S. Tarakanath, Radiation protection of the patient during radiotherapy. *Strahlentherapie* **152**, 191–198 (1976).
11. A. Niroomand-Rad and R. Cumberlin, Measured dose to ovaries and testes from Hodgkin's fields and determination of genetically significant dose. *Int. J. Radiat. Oncol. Biol. Phys.* **25**, 745–751 (1993).
12. S. Mutic and D. A. Low, Whole-body dose from tomotherapy delivery. *Int. J. Radiat. Oncol. Biol. Phys.* **42**, 229–232 (1998).
13. S. Mutic and E. E. Klein, A reduction in the AAPM TG-36 reported peripheral dose distributions with tertiary multileaf collimation. *Int. J. Radiat. Oncol. Biol. Phys.* **44**, 947–953 (1999).
14. S. Mutic, J. Esthappan and E. E. Klein, Peripheral dose distributions for a linear accelerator equipped with a secondary multileaf collimator and universal wedge. *J. Appl. Clin. Med. Phys.* **3**, 302–309 (2002).
15. B. J. McParland and H. I. Fair, A method of calculating peripheral dose distributions of photon beams below 10 MV. *Med. Phys.* **19**, 283–293 (1992).

16. K. R. Kase, G. K. Svensson, A. B. Wolbarst and M. A. Marks, Measurements of dose from secondary radiation outside a treatment field. *Int. J. Radiat. Oncol. Biol. Phys.* **9**, 1177–1183 (1983).

17. D. Greene, P. G. Karup, C. Sims and R. J. Taylor, Dose levels outside radiotherapy beams. *Br. J. Radiol.* **58**, 453–456 (1985).

18. D. Greene, G. L. Chu and D. W. Thomas, Dose levels outside radiotherapy beams. *Br. J. Radiol.* **56**, 543–550 (1983).

19. P. Francois, C. Beurtheret and A. Dutreix, Calculation of the dose delivered to organs outside the radiation beams. *Med. Phys.* **15**, 879–883 (1988).

20. S. Bieri, M. Russo, M. Rouzaud and J. M. Kurtz, Influence of modifications in breast irradiation technique on dose outside the treatment volume. *Int. J. Radiat. Oncol. Biol. Phys.* **38**, 117–125 (1997).

21. C. L. Hartmann Siantar, R. S. Walling, T. P. Daly, B. Faddegon, N. Albright, P. Bergstrom, A. F. Bielajew, C. Chuang, D. Garrett and R. K. House, Description and dosimetric verification of the PEREGRINE Monte Carlo dose calculation system for photon beams incident on a water phantom. *Med. Phys.* **28**, 1322–1337 (2001).

22. D. W. Rogers, B. A. Faddegon, G. X. Ding, C. M. Ma, J. We and T. R. Mackie, BEAM: a Monte Carlo code to simulate radiotherapy treatment units. *Med. Phys.* **22**, 503–524 (1995).

23. A. E. Schach von Wittenau, L. J. Cox, P. M. Bergstrom, Jr., W. P. Chandler, C. L. Hartmann Siantar and R. Mohan, Correlated histogram representation of Monte Carlo derived medical accelerator photon-output phase space. *Med. Phys.* **26**, 1196–1211 (1999).

24. J. Lehmann, R. Stern, J. Levy, T. P. Daly, C. L. Hartmann Siantar and Z. Goldberg, Radiation phantom with humanoid shape and adjustable thickness (RPHAT). *Phys. Med. Biol.* **49**, N125–N129 (2004).

25. D. P. Gierga, J. Brewer, G. C. Sharp, M. Betke, C. G. Willett and G. T. Chen, The correlation between internal and external markers for abdominal tumors: Implications for respiratory gating. *Int. J. Radiat. Oncol. Biol. Phys.* **61**, 1551–1558 (2005).

26. N. Koch, H. H. Liu, G. Starkschall, M. Jacobson, K. Forster, Z. Liao, R. Komaki and C. W. Stevens, Evaluation of internal lung motion for respiratory-gated radiotherapy using MRI: Part I—correlating internal lung motion with skin fiducial motion. *Int. J. Radiat. Oncol. Biol. Phys.* **60**, 1459–1472 (2004).

27. E. Tochilin and P. D. LaRiviere, *Neutron Leakage Characteristics Related to Room Shielding*, pp. 145–154. NBS Special Publication no. 554, National Bureau of Standards, Gaithersburg, MD, 1979.

28. NCRP, *Neutron Contamination from Medical Electron Accelerators.* Report No. 79, National Council on Radiation Protection and Measurements, Bethesda, MD, 1984.

29. O. Chibani and C. M. Ma, Photonuclear dose calculations for high-energy photon beams from Siemens and Varian linacs. *Med. Phys.* **30**, 1990–2000 (2003).

30. R. Barquero, R. Mendez, M. P. Iniguez, H. R. Vega and M. Voytchev, Thermoluminescence measurements of neutron dose around a medical linac. *Radiat. Prot. Dosim.* **101**, 493–496 (2002).